ISA Transactions 53 (2014) 568–577

Contents lists available at ScienceDirect

ISA Transactions

journal homepage: www.elsevier.com/locate/isatrans

Faulty measurement substitution and control reconfiguration by using a multivariate flow control loop

Sergio R.P. Perillo [a], Belle R. Upadhyaya [b,*], J. Wesley Hines [b]

[a] IPEN-CNEN/SP, Sao Paulo, Brazil
[b] Department of Nuclear Engineering, University of Tennessee, Knoxville, TN 37996-2300, USA

ARTICLE INFO

Article history:
Received 12 September 2012
Received in revised form
1 October 2013
Accepted 13 December 2013
Available online 8 January 2014
This paper was recommended for publication by Dr. Karlene Hoo

Keywords:
Measurement substitution
Control reconfiguration
Data-driven models
Fault-tolerant control
Sequential probability ratio test

ABSTRACT

A two-tank multivariate loop was designed and built to support research related to instrumentation and control, equipment and sensor monitoring. This test bed provides the framework necessary to investigate and test control strategies and fault detection methods applicable to sensors, equipment, and actuators, and was used to experimentally develop and demonstrate a fault-tolerant control strategy using six correlated variables in a single-tank configuration. This work shows the feasibility of using data-based empirical models to perform fault detection and substitute faulty measurements with predictions and to perform control reconfiguration in the presence of actuator failure in a real system. These experiments were particularly important because they offered the opportunity to prove that a system, such as the multivariate control loop, could survive degraded conditions, provided the empirical models used were accurate and representative of the process dynamics.

© 2013 ISA. Published by Elsevier Ltd. All rights reserved.

1. Introduction

Several techniques for on-line monitoring of equipment and systems in nuclear power plants are well established. Since the early 1970s, numerous efforts have been made to detect and identify anomalies and to provide alternative ways to measure critical and non-critical operating parameters in power plants, particularly reactor noise analysis which uses existing sensor signals to detect incipient faults, measure sensor response time, identify blockages in sensor lines, vibration of reactor internals, imbalance in rotating machinery, etc. In 1992 an MIT report [1] described the theoretical development and the evaluation via both experiment and simulation of digital methods for the closed-loop control. Signal validation and instrument fault detection was also used in this work by means of a numerical technique called "parity space approach" [2–5], which is based on simple algebraic projections and geometry. This method computes a residual vector that is zero when no fault is present and non-zero otherwise. The residual will also be different for different faults. In addition to validating sensor readings, this methodology performs instrument fault checks in which the weighting factor for each sensor is adjusted in proportion to the frequency with which its readings are judged to be valid. Thus, reliance on a failing sensor is gradually reduced, thereby assuring a "bumpless" transition when complete failure actually occurs. Examples of different techniques in the literature range from using Principal Components Analysis (PCA) [6–12] to Fuzzy Logic, Genetic Algorithm (GA) and Artificial Neural Networks (ANN) [6], to data clustering [8] and other residual generation approaches [13]. In many cases more than one approach were used, sometimes combining several of such approaches as tools to obtain residuals and/or control algorithms. In some works, techniques such as ANN and Group Method Data Handling (GMDH) were merged to form GMDH-Type Neural Network Algorithms [14–17] to help predict values based on historical data.

Such techniques evolved into on-line monitoring to track the vibration of reactor internals, measure reactor stability, verify overall plant thermal performance, leak detection, estimation of remaining useful life of equipment, and others. Early detection of the onset of equipment and instrument channel degradation and failure can improve plant safety, prevent loss of operational capability, reduce radiation exposure of plant personnel, enhance plant control, and minimize repair time [18].

The development of an on-line approach for monitoring and control with application to an experimental flow loop is described in this work, corroborating results available in the literature suggesting the applicability of such approach to operating plants with appropriate data acquisition and analytical redundancy. The approach uses empirical, data-based methods for characterizing the relationship among a set of measurements as data sets often

* Corresponding author. Tel.: +1 865 974 7576; fax: +1 865 974 0668.
E-mail address: bupadhya@utk.edu (B.R. Upadhyaya).

0019-0578/$ - see front matter © 2013 ISA. Published by Elsevier Ltd. All rights reserved.
http://dx.doi.org/10.1016/j.isatra.2013.12.013

contain much more information than can be learned from just looking at plots of those data. Models based on observed input/output data can help us abstract and gain new information and understanding from these data sets. They can also serve as substitutes for more process-based models in applications where computational speed is critical or where the underlying relationships are poorly understood.

2. Description of the experimental flow control loop

The two-tank flow facility was constructed on a wheeled table-like steel frame structure seven-foot long, four-foot wide and six-foot high. This structure holds all sensors, piping, pump, sump tank, aircraft aluminum table top, cables, control valves, manual valves, connection boxes, power strips, and two tanks all of which can be repositioned. Since about 80% of the piping used to build the loop is made of Chlorinated Polyvinyl Chloride (CPVC) or PVC, union connections were strategically distributed so any maintenance or minor setup modification can easily be carried out. In Fig. 1 the final layout with both acrylic tanks is shown.

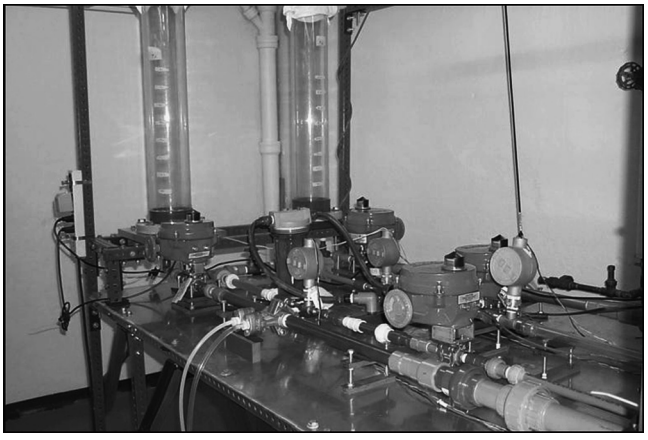

Fig. 1. Final layout of the control loop.

Level control experiments utilize two similar acrylic tanks, referred to as Tank 1 and Tank 2, respectively, and their dimensions are 146 mm in diameter and 1 m long. A 102-l stainless steel tank is installed underneath the table top to provide the necessary water for the circuit.

Several sensors for process measurement are installed in the loop: differential pressure transmitters, thermocouples, turbine flow meters, orifice meters and signal conditioners.

In order to manipulate the water flowing in the loop, five control valves are used: one at each tank inlet, one at each tank exit, and one connecting the piping between the tanks. These control valves have two components: an electric actuator and a 12.7 mm (½″) ball valve. Although not all five motor-operated valves (MOV) are actually used for control purposes, these actuators are manipulated via software and are responsible for opening and closing the ball valves to regulate the flow according to the experiment being carried out. The actuators are 120 VAC powered, with input and output of 2–10 VDC and can be locally or remotely operated, with a typical stroke time of 15 s (stroke time is the time needed to move the valve from the fully closed to fully open position, and conversely).

3. Description of the control loop devices and instrumentation

The two-tank loop was built primarily to provide the necessary framework to develop research related to instrumentation and control strategies, equipment and sensor monitoring, model-predictive control, and the demonstration of fault detection and fault-tolerant control strategy and reconfigurable control. With such objectives in mind, a set of sensors and actuators were placed in key positions throughout the loop to monitor and manipulate the water flow circulating in the loop. Fig. 2 depicts a schematic of this loop with low-pressure water circulation that is facilitated by a fractional horsepower motor-driven pump.

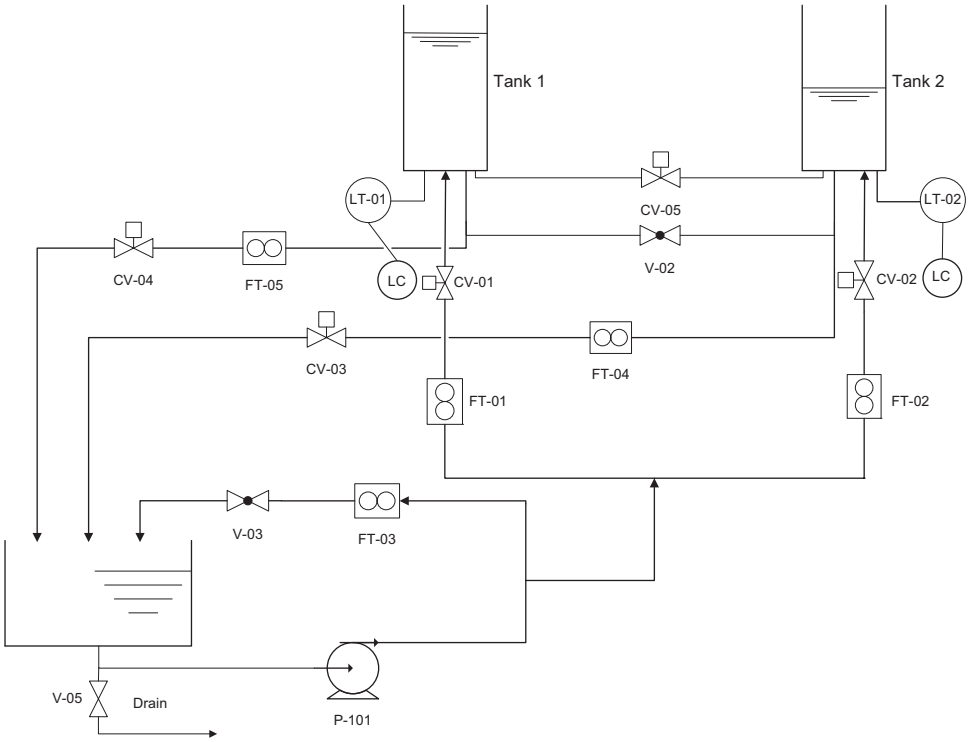

Fig. 2. Schematic of the two-tank experimental control loop.

The sensors are identified as follows:

LT-XX:Level transmitter
LC-XX:Level control
CV-XX: Control valve
FT-XX: Flow rate meter
V-XX: Manual valve
P-101: Centrifugal pump

The loop has a centrifugal pump, one stainless steel water reservoir, two acrylic tanks, four flow meters, two level transmitters, five motor-operated control valves (MOV), and three manual valves. The piping is made of either CPVC schedule 80 or PVC, with diameters varying from 38 mm to 12.7 mm (1–1/2″ to ½″) and provides flexibility to accommodate minor design changes. A data acquisition and control system developed especially for this loop is used to monitor and control the loop by varying the position of two control valves until a stationary flow throughout the system as well as a pre-set water level in either one or both acrylic tanks is attained. An MOV in between tanks provides the capability to work with both acrylic tanks (connected or not) at the same time.

A bypass valve is provided to divert the excess water back to the water reservoir and lower the pressure in the loop. The maximum rated water flow is estimated to be around 2 l/s (32 GPM), provided the necessary pump pressure head is met. Though water temperature is monitored, temperature control is not performed but changes can be implemented for this purpose. The 1.2 m wide, 2.1 m long and 1.8 m high steel frame supports the equipment, up to a maximum load of approximately 360 kg.

4. Data acquisition system

In order to perform the various experiments using the loop, a few human–machine software interfaces, called Virtual Instruments (VIs), were developed using the National Instruments LabVIEW®-based package and data acquisition (DAQ) hardware. These VIs are capable of controlling the loop in both manual and automatic modes while performing data acquisition, monitoring, and logging the data in computer files for later use. Both software and hardware used in the two-tank loop are discussed next.

Two different data acquisition (DAQ) cards are installed in the personal computer used to run the loop, and are used for data acquisition/control purposes, and both are manufactured by National Instruments.

The first card is a 16-bit PCIe-6259 with 32 analog inputs and four analog outputs channels. This is a fast card capable of acquiring data at a speed of 1 MS/s (mega-samples per second) for multi-channels (1.25 MS/s for one channel), and output update speed of 2.86 MS/s. The second card is a 12-bit PCI-MIO-16E-4 (discontinued) now known as PCI-6040E with 16 analog inputs and two analog outputs, capable of acquiring data at 500 kS/s (for one channel) or 250 kS/s for multiple channels, and output update speed of 1 MS/s.

Three NI SCB-68 patch panels are used to connect the data acquisition cards to the various sensors and actuators installed in the loop. The NI SCB-68 is a shielded I/O connector block for interfacing I/O signals to plug-in data acquisition (DAQ) devices with 68-pin connectors. Combined with the shielded cables, the SCB-68 provides rugged, very low-noise signal termination, and it has an onboard cold-junction compensation sensor for low-cost

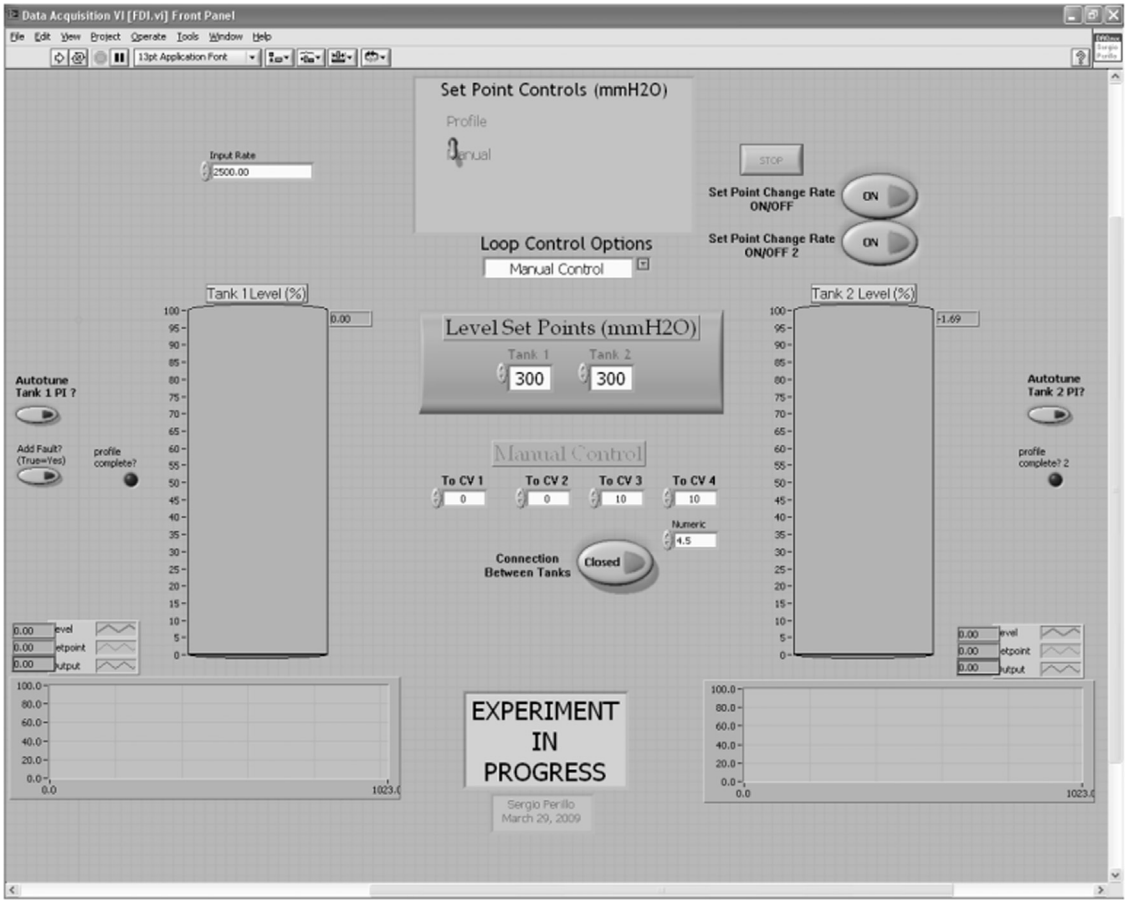

Fig. 3. Control VI front panel showing the manual control option.

thermocouple measurements. The analog outputs from these panels are used to control the MOVs through a hand-made CPVC box.

Due to the higher sampling rate speed of the PCIe-6259 card and the greater number of input channels available, it was selected to be used as the hardware interface controller with the loop, whereas the second card, the PCI-MIO-16E-4 is basically used for data acquisition monitoring and data logging, though it is also used to open or close the two control valves installed at the exit of the tanks.

The first VI runs on the fastest DAQ and it holds all the control logic, control options (manual or automatic) for either Tank 1, Tank 2, both tanks operating together, tanks connected or disconnected, set point control options (manual or pre-set profile), controlled fault insertion (bias or drift), set point rate control, proportional-integral (PI) control gains for each tank separately and/or connected and gain optimization options using the auto-tune feature provided by LabVIEW, and many other functions. It also contains the MATLAB m-file code that provides the expected values used in the fault detection feature when running in Tank 1-only mode. The front panel automatically changes its appearance based on the configuration of the experiment being performed. Two different front panels are shown in Figs. 3 and 4, respectively. The first panel in Fig. 4 shows the typical configuration when the loop is running in manual control using both tanks, either disconnected or not. A push button located right underneath the MOV manual control input boxes opens or closes the MOV connecting both tanks. A second panel is shown in Fig. 4 with the typical configuration when the loop is running in automatic control using PI and Tank 2. Note that all controls related to Tank 1 are no longer present.

The VIs developed to monitor, control and store data acquired from the loop are based on National Instruments LabVIEW, which is a graphical programming environment used to develop sophisticated measurement, test, and control systems using intuitive graphical icons and wires that resemble a flowchart. Two main VIs were developed for the purpose of monitoring the dynamic condition by showing the current engineering values of all significant variables in SI (International System of Units), storing the data and controlling the two-tank loop and are described next.

The second VI runs on the second, slower DAQ, and serves a dual purpose: it is used for monitoring the loop dynamic condition by showing the current engineering values of all significant variables and comparing some of these variables to the expected values (for one single tank) generated in the first VI, and is used to acquire and store the data files on the computer for later use. The current file format used for saving the files is ASCII, which can be imported from and read by a plethora of different software packages. All flow rate equations from turbine and orifice flow meters and unit conversions are located in this VI. All main loop values are monitored and are shown in the main VI panel depicted in Fig. 5.

5. Analytical tools for developing the empirical models

5.1. Principal component analysis

Principal Component Analysis (PCA) is a multivariate method used to capture the relationships in the data while reducing the dimensionality of an input space without losing a significant

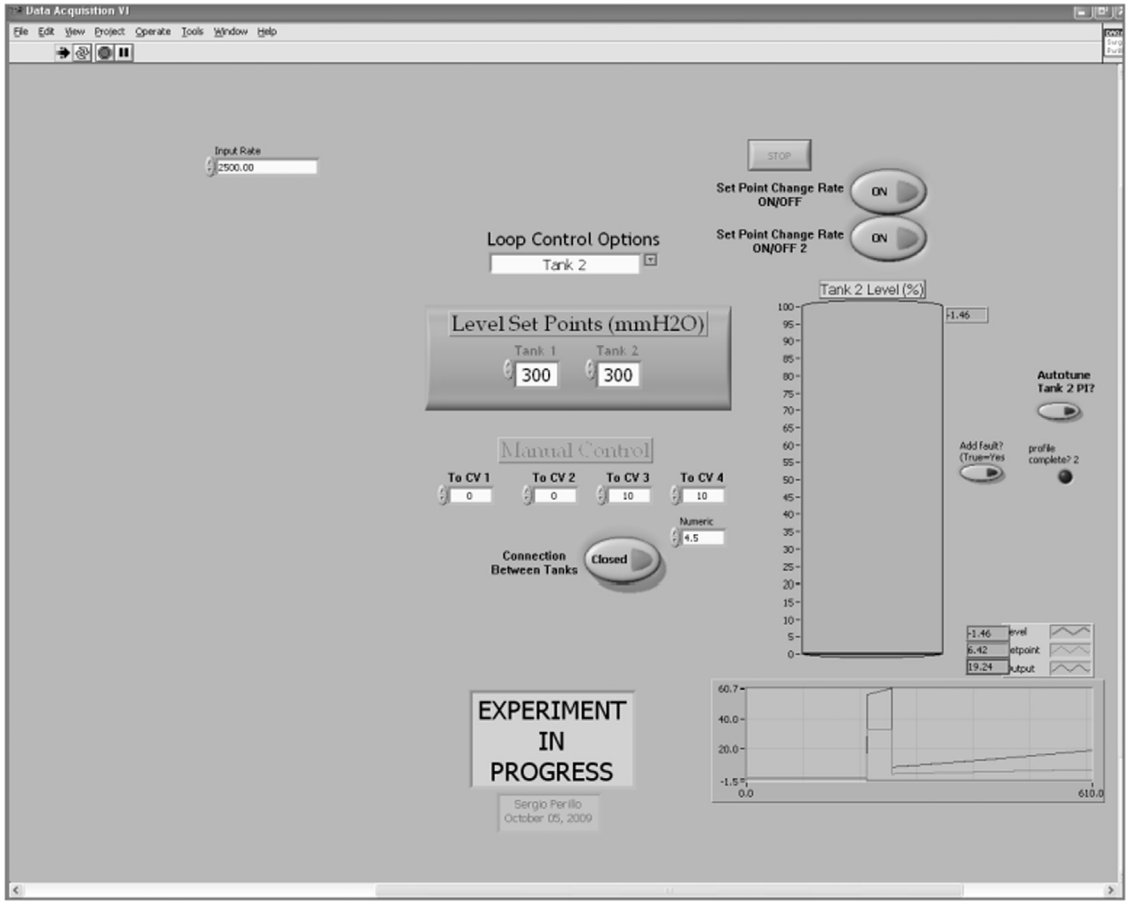

Fig. 4. Control VI front panel showing the automatic control for Tank 2.

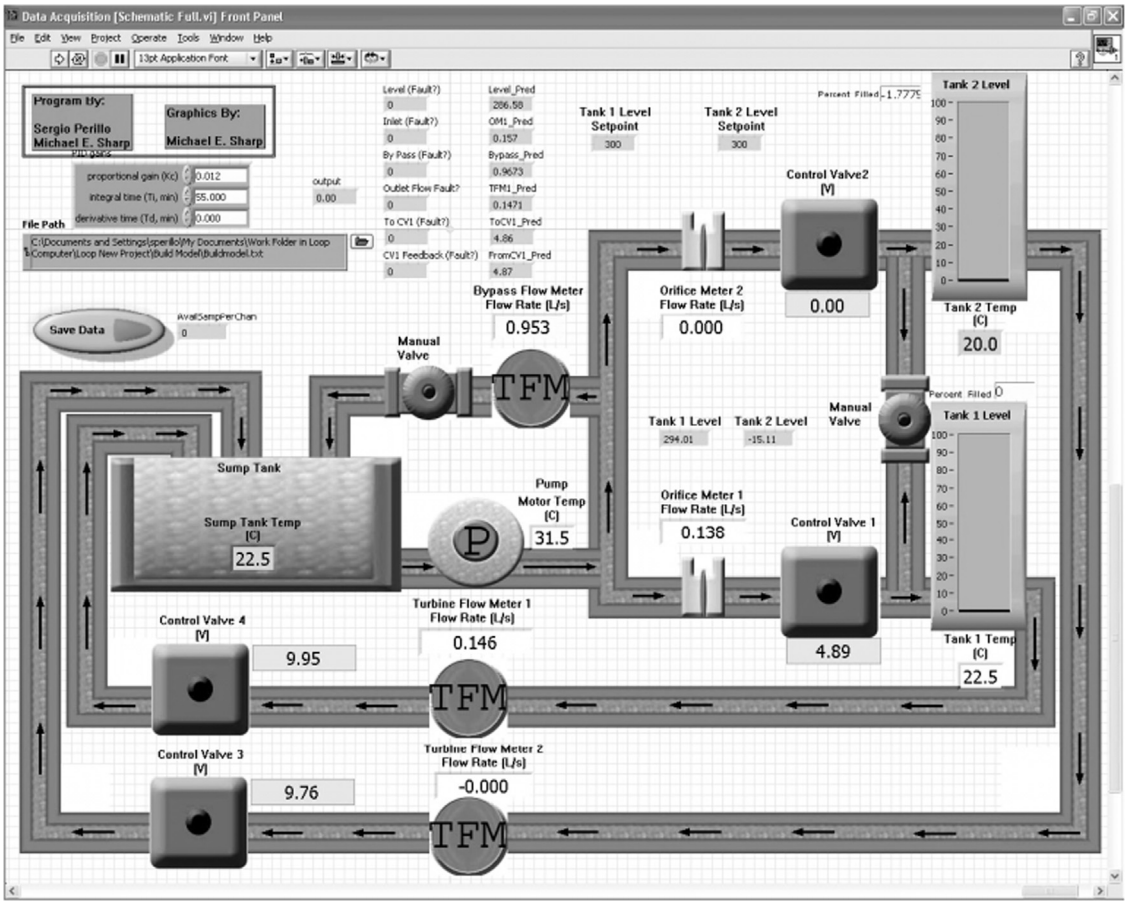

Fig. 5. Data acquisition main panel.

amount of information (variability). The method also makes the transformed vectors orthogonal and uncorrelated and is particularly useful for analysis of ill-conditioned data; hence such transformed vectors can be used by regression techniques without having the problems of co-linearity. A lower dimensional input space will also usually reduce the time necessary to train a data-based model and the reduced noise will improve the mapping. The objective of PCA is to reduce the dimensionality and preserve as much of the relevant information as possible. PCA can also be thought of as a method of preprocessing data to extract uncorrelated features from the data. Further details can be found in [18,19].

5.2. Auto-associative kernel regression (AAKR)

AAKR is a non-parametric, empirical modeling technique that uses historical, fault-free observations and can be used to correct any errors present in current observations. Further details can be found in [20].

5.3. Sequential probability ratio test (SPRT)

The method chosen to detect faults in sensors and actuators in this work was the SPRT, and is based on the assumption that the residuals of a model are normally distributed and uncorrelated. This method, which was originally developed by Wald [21] and applied by many investigators [20,22], detects changes in signal properties, such as mean and standard deviation of a signal, and is used to identify drifts and changes in noise levels, while minimizing the probability of false alarms.

When performing a hypothesis test between two point hypotheses, the likelihood-ratio test is the most powerful test of size α for a threshold η. So, when

$H_0 : \theta = \theta_0$, and $H_0 : \theta = \theta_1$ the likelihood ratio test rejects the null hypothesis H_0 when,

$$\Lambda(x) = \frac{L(\theta_0 | x)}{L(\theta_1 | x)} \leq \eta \quad \text{where } P(\Lambda(x) \leq \eta | H_0) = \alpha \tag{1}$$

Given the likelihood equation P with residuals s_k at time k and mean m_i and variance σ_i for hypothesis I, the likelihood ratio is

$$\lambda_k = \frac{P_1(s_k, m_1, \sigma_1)}{P_0(s_k, m_0, \sigma_0)} \tag{2}$$

The log likelihood ratio becomes

$$\lambda_k = \ln(\lambda_k) = \ln\left[\frac{P_1(s_k, m_1, \sigma_1)}{P_0(s_k, m_0, \sigma_0)}\right] = \sum_{i=1}^{k} \ln\left[\frac{P_1(s_i, m_1, \sigma_1)}{P_0(s_i, m_0, \sigma_0)}\right] \tag{3}$$

This can be written in the recurrent form as

$$\lambda_k = \lambda_{k-1} + \ln\left[\frac{P_1(s_i, m_1, \sigma_1)}{P_0(s_i, m_0, \sigma_0)}\right] \tag{4}$$

Assuming Gaussian distribution of the residual sequence $\{s_k\}$, Eq. (4) is written as

$$\lambda_k = \lambda_{k-1} + \ln\left[\frac{\frac{1}{\sqrt{2\pi\sigma_1^2}}\exp\left[-\frac{(s_k - m_1)^2}{2\sigma_1^2}\right]}{\frac{1}{\sqrt{2\pi\sigma_0^2}}\exp\left[-\frac{(s_k - m_0)^2}{2\sigma_0^2}\right]}\right] \tag{5}$$

This facilitates expressing Eq. (5) in the following algebraic form:

$$\lambda_k = \lambda_{k-1} + \ln\left(\frac{\sigma_1}{\sigma_0}\right) + \frac{(s_k - m_0)^2}{2\sigma_0^2} - \frac{(s_k - m_1)^2}{2\sigma_1^2} \quad (6)$$

The residual distributions can be assumed to be normally distributed with zero mean and same variance, so Eq. (6) becomes

$$\lambda_k = \lambda_{k-1} + \frac{m_1}{\sigma^2}\left(s_k - \frac{m_1}{2}\right) \quad (7)$$

Using Wald's two-sided test A and B are defined as

$$A = \ln\left(\frac{\beta}{1-\alpha}\right) \text{ and } B = \ln\left(\frac{1-\beta}{\alpha}\right) \quad (8)$$

where:

α is the probability of false alarm, and should be kept small to avoid a Type I error, or false positive.

β is the probability of missing an alarm for a Type II error, or false negative.

The status of the equipment being monitored is determined by a comparison of A and B with the log likelihood ratio, i.e.:

For $\lambda_m < A$ the sensor can be considered in good condition.

For $\lambda_m > B$ the sensor can be considered degraded.

As depicted in Fig. 6, rather than computing a new mean and variance at every new sample acquired, the SPRT monitors the equipment's performance by processing the residuals in a sequential fashion. The residual signals, which are the differences between the sensor measurements and the estimates from the model, are used to generate a likelihood ratio (ratio of joint probability density of residuals) based on the statistical properties of the incoming data compared with the statistics in the model. In other words, based on the statistics of the new data coming from the equipment being monitored, the method is capable of detecting differences in such statistical properties and inform if the new data comes from a similar statistical distribution or not. This process of comparing the model predictions with values coming from the equipment is depicted in Fig. 7, where the likelihood ratio is evaluated by the SPRT threshold for the specified component to make a logical decision concerning its status.

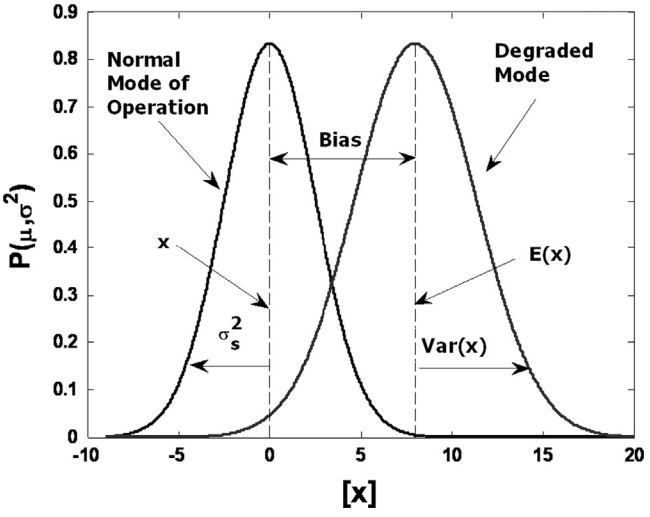

Fig. 6. The SPRT is based on comparing statistical differences.

5.4. Process and equipment monitoring (PEM) toolbox

On-line monitoring commonly uses an auto-associative empirical modeling architecture to assess equipment performance. An auto-associative architecture predicts a group of correct sensor values when supplied a group of sensor values that is usually corrupted with process and instrument noise, and could also contain faults such as sensor drift or complete failure. The PEM Toolbox [23,24], which was developed at The University of Tennessee, is a set of MATLAB based tools, which have been developed to support the design of process and equipment condition monitoring systems. Its purpose is to provide the necessary tools so that different empirical modeling and uncertainty estimation methods may be easily investigated and compared. In this research several PEM toolbox functions were used to obtain the empirical models necessary to perform fault detection using the sensors and actuators measurements installed in the loop, and as such, some stand-alone, low-level PEM-based functions are currently implemented in the data acquisition VI to monitor and compare measurements and predictions.

6. Data generation and model development

A 2.5 h long dataset with level set points varying from 300 mmH_2O to 600 mmH_2O, containing 10 variables for a single-tank configuration was acquired and used to obtain the empirical models, based on the PCA findings. Each model used variables that are correlated with each other based on their loadings, but making sure at least one not-so-much correlated variable was included in the model to provide the necessary robustness to the fault detection routine currently incorporated in the data acquisition VIs, although risking an increase in model bias. This trade-off is particularly important in obtaining models that will be used for fault detection. For instance, the outlet flow rate is highly correlated with the water level in the tank, and this variable alone would be enough in the model to predict water level. But if the water level is to be inferred using faulty outlet flow rate sensor readings the predictions would be incorrect, but by including the inlet flow rate readings such one-on-one variable dependency can be diminished, hence adding some robustness to the model.

Three different models were investigated for each of the six variables: linear regression, kernel regression and AAKR, and the final models implemented in the routine responsible for the fault detection were chosen based upon their Mean Absolute Percent

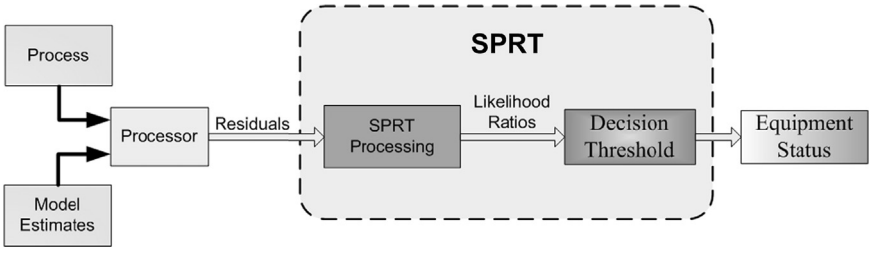

Fig. 7. Diagram showing the implementation of SPRT.

Error (MAPE), defined as

$$MAPE = \frac{1}{n}\sum_{i=1}^{n}\left|\frac{\text{Actual}(i) - \text{Predicted}(i)}{\text{Actual}(i)}\right| \quad (9)$$

where n is the number of fitted points and i corresponds to the i-th value

Fig. 8 shows MAPE values for all three different modeling methods investigated: linear and kernel regressions, and AAKR. In three of the cases, inlet flow rate control and control valve feedback signals, the regression models performed just as well as the AAKR models, while linear regression worked well for four variables, outperforming both AAKR and linear. In the case of the inlet flow rate the AAKR model outperformed the other two models, in great part due to non-linearity caused by the control valve hysteresis. All bypass models presented the lowest MAPE of all, with less than 0.5%. In this case the linear model was chosen for being the least complex model of all three. In conclusion, five linear regression and one AAKR models were chosen to be used to perform the predictions and fault detection.

After the empirical models were obtained they were implemented in the data acquisition VI and a different dataset was acquired using the same set points as the original dataset used to obtain the models. The new measurements were used as queries to the models, and the results comparing the predicted values with the new query are shown in Figs. 9–12. Noteworthy are the level predictions in Fig. 10 with an average absolute deviation from measured values of about 30 mmH_2O, and maximum of 40 mmH_2O, and the tank outlet flow rate with an average deviation of about 3×10^{-3} l/s. Bypass predictions deviations were also very low around 2% of maximum flow rate (0.92 l/s). The inlet flow rate showed a high absolute difference of about 26% or 0.04 l/s with maximum flow rate of around 0.152 l/s, greatly due to the control valve non-linearity.

7. Fault detection and measurement substitution

The water level in the tank is measured by a pressure sensor installed at the bottom of the tank and is regulated by varying the volume of water entering and exiting the tank at any given time. By default and under normal operation, the tank exit control valve is left open so that the inlet flow rate control valve is fully responsible for controlling the water level in the tank and any undue changes in the level measurement affect the PI

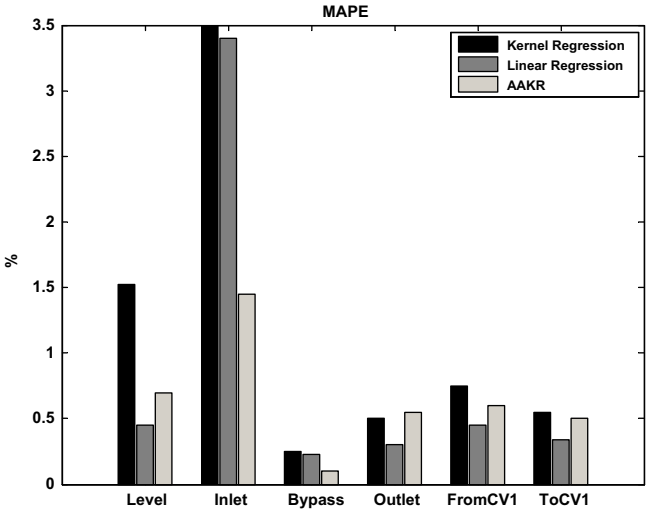

Fig. 8. MAPE for linear regression, kernel regression, and AAKR models.

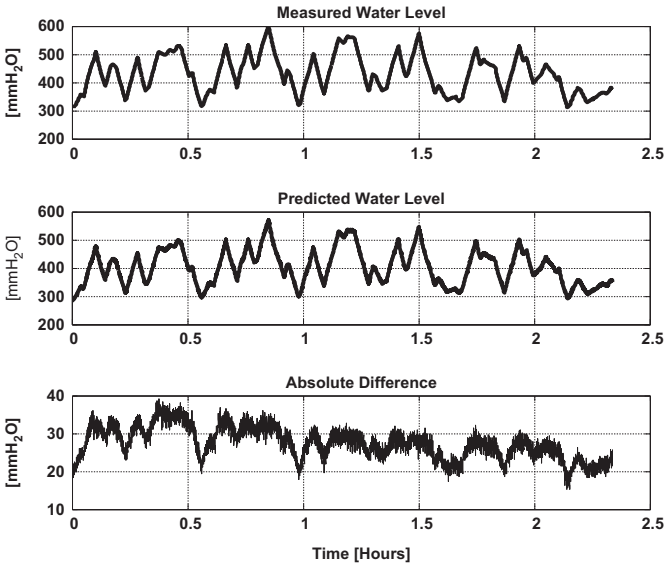

Fig. 9. Measured water level versus predicted values.

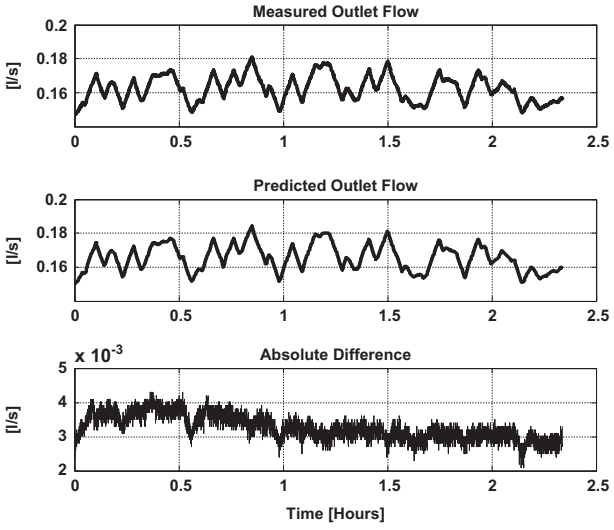

Fig. 10. Measured outlet flow rate versus predicted values.

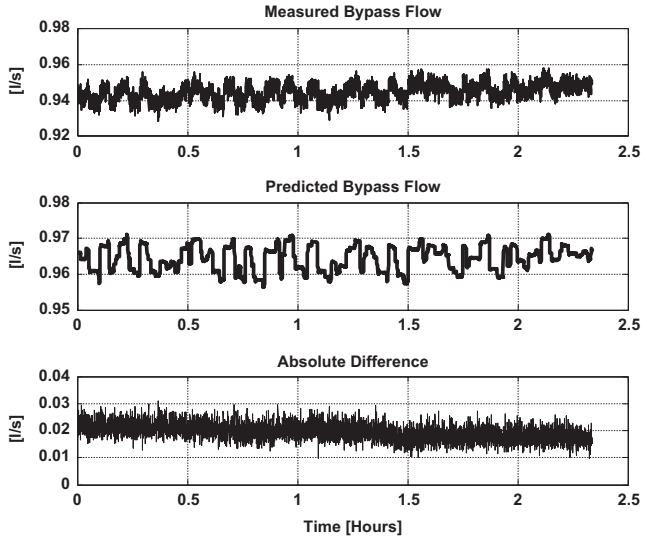

Fig. 11. Measured bypass flow rate versus predicted values.

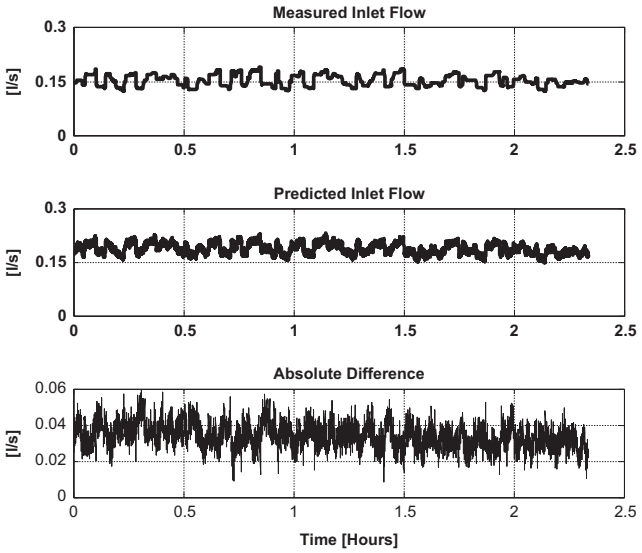

Fig. 12. Measured inlet flow rate versus predicted values.

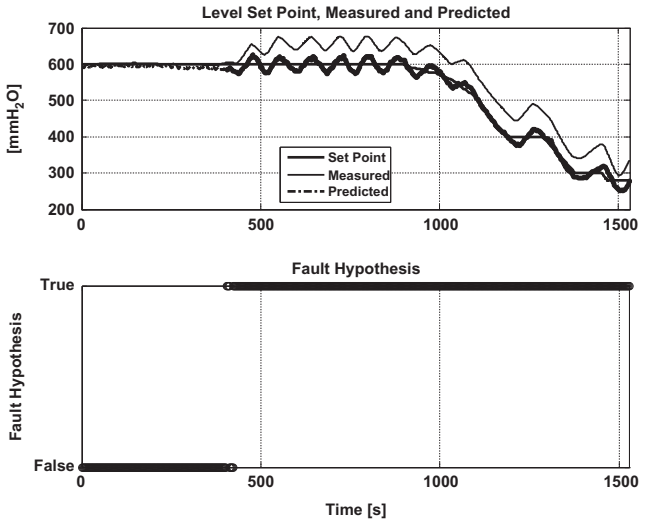

Fig. 13. Faulty level measurement substitution.

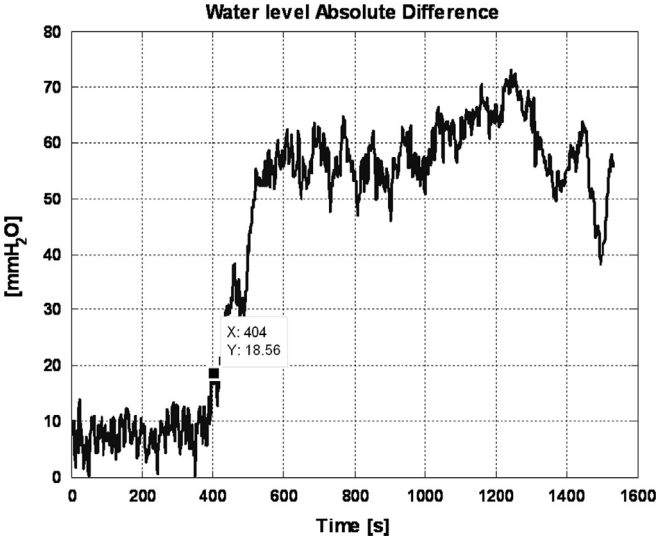

Fig. 14. Water level absolute difference for slow changing drift.

(Proportional-Integral) controller output signal sent to the control valve. Hence a 2 in 1 experiment was performed to test the fault detection capability and faulty measurement substitution by first adding a positive drift of 50 mm-H_2O over 3 min to the water level measurement sensor and changing the level set point thereafter.

With empirical models and SPRT continuously running and monitoring each acquired level measurement, and comparing its value to predicted values it was possible to identify each measurement as belonging to either a faulty or a non-faulty condition. When the residuals between prediction and measurement exceeded a pre-determined threshold, based on the statistical properties of the dataset used to obtain each of the empirical models, the SPRT flagged that measurement, indicating a faulty condition. Once the faulty condition was detected, the faulty measurements used as inputs to both controller and empirical models were automatically substituted with predicted values generated by the level model alone. However, shortly after the faulty measurements were substituted with predictions, the empirical models misidentified the new situation as being non-faulty and switched back to the faulty measurements coming from the sensor. This situation caused the system to keep switching back and forth, oscillating between faulty and non-faulty modes. To avoid such a problem, a "latch-on" control was added to the fault detection routine, keeping the system from going back to normal condition after identifying and replacing the faulty measurements.

The results from the experiment are shown in Fig. 13. The dotted line at the start of the experiment at steady state are predictions being provided by the fault detection module, and measurements substituted with predictions are shown in thick solid line after a faulty condition was identified. In this experiment, once the difference between measured and predicted values reached around 18 mmH_2O, the level SPRT triggered changing from normal to faulty condition (Fig. 14), causing measured values to be substituted with predicted values, therefore isolating the faulty sensor from the loop. The outlet flow rate model was also able to detect the fault a few seconds later, but not the inlet flow rate until later in the experiment. The controller had difficulties using the prediction values, in large part due to how both VIs were set up and data were transferred between them; but once the PI gains were tuned, the controller was able to successfully change the water level from 600 to 300 mmH_2O, although with some performance degradation, showing the applicability of this method for slow-changing processes. Fig. 15 shows the inlet flow rate valve position (0 V closed and 7 V fully open).

It is important to acknowledge that, since the multivariate loop is an open process, meaning the water inventory in the water reservoir varies over time due to small leaks and evaporation, the empirical models were obtained under well-controlled conditions, and are valid only within the range of operation the data was acquired. Any significant deviations from such conditions will cause the predictions to diverge from measurements, causing the fault detection routine developed to misidentify the measurements as coming from a faulty condition.

This experiment involved detecting a fault in the water level due to a fault in the flow rate control valve and automatically open the valve connecting both tanks while switching the control action to the second tank inlet control valve, therefore sending the error difference signal between set point and measured water level to the second tank inlet flow rate controller and have it control the water level in the first tank by varying its own level.

Initiating the experiment, the single-tank configuration was running around steady state at 500 mmH_2O, and at a certain point in time the control output was overridden by a 4.5 V signal sent to the control valve, causing the water level to deviate from the set point.

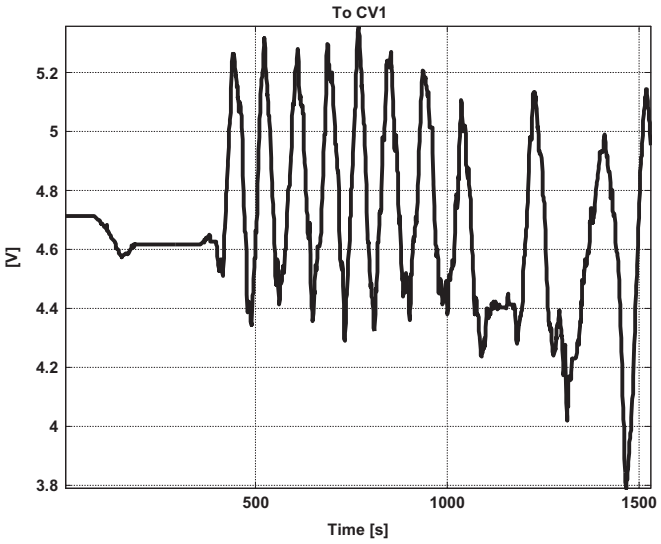

Fig. 15. Inlet flow rate valve position.

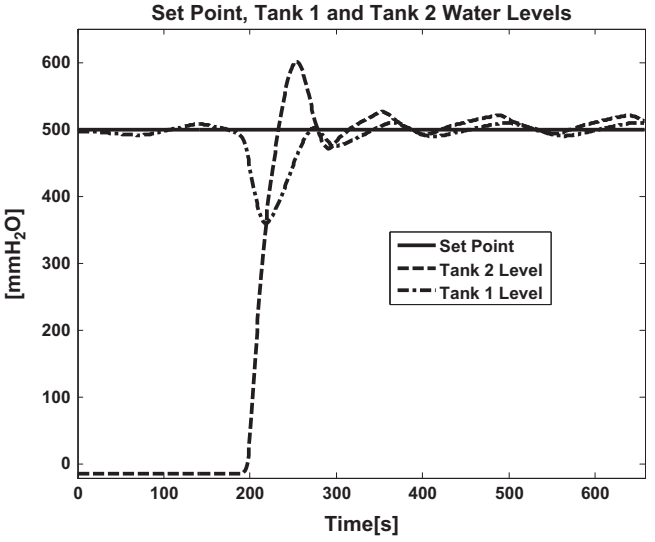

Fig. 16. Inlet flow rate control valve position at 4.5 V with control switched over to tank 2.

8. Application of reconfigurable control to the flow loop

With the control valve stuck at 4.5 V there was not an initial increase in the water level as can be seen in Fig. 16. The sharp drop in level is due to the connection between tanks being opened with tank 2 empty. The water level measurements with the water level in tank 1 showed a 10 mmH_2O average overshoot with respect to the set point, but still presenting the oscillating condition around set point, with 140 s cycles, the same occurring with the tank 2 level measurements. Since the departure from normal condition started at the same voltage needed to achieve 500 mmH_2O in the tank, the inlet flow rate model took 60 s longer and it flagged the faulty condition when the difference between measured and predicted values reached 22 mmH_2O, compared to the 20 s needed by the level, bypass and outlet flow rate to detect the same fault.

About 10 s after the fault was introduced (logic 10 out of 10), the SPRT flagged the control output as being faulty and immediately opened the control valve that connects both tanks, while at the same time opened both inlet and outlet flow rate control valves to the second tank and transferred the control from the first to the second tank.

9. Concluding remarks

The objective of this work and development was to show the feasibility of using fault detection using data-based empirical models, fault identification, and automated sensor replacement to substitute faulty measurements with predictions and perform control reconfiguration in the presence of actuator failure in a real system. For this purpose a multivariate loop was used in single-tank configuration where six empirical models were developed. Level measurements were successfully substituted with predictions and provided the system the necessary flexibility to continue operation even under degraded conditions, thus offering survivability of the system and the time necessary to perform corrective procedures, should that be the necessary. These experiments were particularly important because they offered the opportunity to prove that a system, such as the multivariate control loop can survive degraded circumstances, provided the empirical models used are accurate and representative of the system dynamics.

Simple variable measurement substitution, not involving control, proved to be a straightforward approach, but special attention was needed to make sure the fault detection system latched on and did not default to normal condition. However, in the second scenario where the variable measurements were used in the single-tank control logic configuration, the time it took for the fault to be detected depended not only on variable correlation but also on the severity of the fault. In addition, some operational peculiarities, such as having dead-band implemented in the water level error signal sent to the PI controller and high-speed rate control loop (2.5 kHz) using model predictions generated at much lower rate (1 Hz) prevented the controller output from adjusting the inlet flow rate control valve faster. In this case the faulty level measurement substitution caused some control instabilities, which required controller re-tuning; but in the end the single-tank was successfully controlled, as the results have shown, with the water level closely following the set points changes. Though this is a slow-transient, non-critical safety system, the important point in this demonstration was to show that a system could have some level of survivability under degraded conditions, provided there is enough analytical and/or physical redundancy. It is important to keep in mind that other safety critical control systems present in airplanes, spacecraft, ships, robots, etc., do have the necessary (hardware) control redundancy to provide them with means to survive system faults.

An important fact to be aware of when using empirical models in real systems, such as the single-tank experimental loop, is that some of the solutions presented here are system/fault dependent and appropriate fault detection techniques such as expert systems need to be employed to properly identify fault scenarios in order to select the appropriate solution.

Acknowledgments

This research was supported by a U.S. Department of Energy NERI-C grant with the University of Tennessee, Knoxville. The authors wish to thank the reviewers for their comments that helped to improve the quality of the manuscript.

References

[1] Bernard, J.A., A. F. Henry, D.D. Lanning, and J.E. Meyer Studies on the closed-loop digital control of multi-modular reactors, Report No. MITNRL-049, Massachusetts Institute of Technology, November, 1992.

[2] Desai, M., A. Ray, A fault detection and isolation methodology, in: Proceedings of the twentieth IEEE conference on decision and control including the symposium on adaptive processes, 1981 Vol 20 Part 1, December 1981, pp 1363–9.

[3] Hagenblad, A., F. Gustafsson, and I. Klein, A comparison of two methods for stochastic fault detection: the parity space approach and principal components analysis. In: Thirteenth IFAC symposium on system identification, 2003.
[4] Upadhyaya BR. Sensor failure detection and estimation. Nucl Saf 1985;26 (1):32–43.
[5] Zhao K, Upadhyaya BR, Wood RT. Robust dynamic sensor fault detection and isolation of helical coil steam generator systems using a subspace identification technique. Nucl Technol 2006;153(3):326–40.
[6] Na MG, et al. Failure detection using a fuzzy neural network with an automatic input selection algorithm. Power Plant Surveill Diagn 2002;14:221.
[7] Kaistha N, Upadhyaya BR. Incipient fault detection and isolation of field devices in nuclear power systems using principal component analysis. Nucl Technol 2001;136(2):221–30.
[8] He QP, Wang J, Qin SJ. A New fault diagnosis method using fault directions in fisher discriminant analysis. AIChE J 2005;51(2):555–71.
[9] Dunia R, Qin SJ. Joint diagnosis of process and sensor faults using principal component analysis. Control Eng Pract 1998;6(4):457–69.
[10] R. Dunia and S. J. Qin, "Multi-dimensional fault diagnosis using a subspace approach," American Control Conference, 1997.
[11] Dunia R, Qin SJ. Subspace approach to multidimensional fault identification and reconstruction. AIChE J 2004;44(8):1813–31.
[12] Dunia R, Qin SJ. A unified geometric approach to process and sensor fault identification and reconstruction: the unidimensional fault case. Comput Chem Eng 1998;22(7–8):927–43.
[13] Patton, R.J., and J. Chen, A review of parity space approaches to fault diagnosis, IFAC SAFEPROCESS symposium, Baden-Baden, 1991.
[14] Kondo Tadashi, Ueno J. Revised GMDH-type neural network algorithm with a feedback loop identifying sigmoid functional neural network. Int J Innov Comput, Inform Control ICIC Int 2006;2(5):985–96.
[15] T. Kondo and A.S. Pandya GMDH-type neural networks with a feedback loop and their application to the identification of large-spatial air pollution patterns. In: Proceedings of the thirty-ninth sice annual conference international session papers, 112A-4, p.1–6, 2000.
[16] Fujimoto Koji, Nakabayashi S. Applying GMDH algorithm to extract rules from examples. Syst Anal Model Simul 2003;43(10):1311–9.
[17] A. Kuzmenko and N. Zagoruyko Structure relaxation method for self-organizing neural networks. In: Proceedings of the seventeenth international conference on pattern recognition, vol. 4, p. 589–592, Aug. 2004.
[18] On-line monitoring for improving performance of nuclear power plants part 1: instrument channel monitoring; Part 2: process and component monitoring and diagnostics; IAEA Technical Report, NP-T-1.1 and NP-T-1.2, 2008.
[19] Kaistha N, Upadhyaya BR. Incipient fault detection and isolation of field devices in nuclear power systems using principal component analysis. Nucl Technol 2001;136:221–30.
[20] Hines JW, Garvey DR. Development and application of fault detectability performance metrics for instrument calibration verification and anomaly detection. J Pattern Recognit Res 2006;1:2–15.
[21] Wald A. Sequential tests of statistical hypotheses. Ann Math Stat 1945;16:117–86.
[22] B.R. Upadhyaya et al., Development and testing of an integrated signal validation system for nuclear power plants, DOE/NE/37959-24, Research Report prepared for the U. S. Department of Energy, September 1988.
[23] J.W. Hines, D.R. Garvey, R. Seibert, and A. Usynin, Technical review of on-line monitoring techniques for performance assessment: theoretical issues, NUREG/CR-6895, vol. 2, University of Tennessee, Knoxville, May 2008.
[24] J.W. Hines and D.R. Garvey, Development of a process and equipment monitoring (PEM) toolbox and its application to sensor calibration monitoring. In: Fourth international conference on quality and reliability (ICQR4), Beijing, China, August 2005.